J. Fluid Mech. (2000), *vol.* 406, *pp.* 175–198. Printed in the United Kingdom

Non-axisymmetric vortices in two-dimensional flows

By STÉPHANE LE DIZÈS

Institut de Recherche sur les Phénomènes Hors Équilibre, 12, avenue Général Leclerc, F-13003 Marseille, France

(Received 14 June 1999 and in revised form 4 October 1999)

Slightly non-axisymmetric vortices are analysed by asymptotic methods in the context of incompressible large-Reynolds-number two-dimensional flows. The structure of the non-axisymmetric correction generated by an external rotating multipolar strain field to a vortex with a Gaussian vorticity profile is first studied. It is shown that when the angular frequency w of the external field is in the range of the angular velocity of the vortex, the non-axisymmetric correction exhibits a critical-point singularity which requires the introduction of viscosity or nonlinearity to be smoothed. The nature of the critical layer, which depends on the parameter $h = 1/(Re\ \varepsilon^{3/2})$, where ε is the amplitude of the non-axisymmetric correction and Re the Reynolds number based on the circulation of the vortex, is found to govern the entire structure of the correction. Numerous properties are analysed as w and h vary for a multipolar strain field of order $n = 2, 3, 4$ and 5. In the second part of the paper, the problem of the existence of a non-axisymmetric correction which can survive without external field due to the presence of a nonlinear critical layer is addressed. For a family of vorticity profiles ranging from Gaussian to top-hat, such a correction is shown to exist for particular values of the angular frequency. The resulting non-axisymmetric vortices are analysed in detail and compared to recent computations by Rossi, Lingevitch & Bernoff (1997) and Dritschel (1998) of non-axisymmetric vortices. The results are also discussed in the context of electron columns where similar non-axisymmetric structures were observed (Driscoll & Fine 1990).

1. Introduction

Recent experiments and numerical simulations have provided evidence of the existence of long-lived non-axisymmetric vortices in large-Reynolds-number two-dimensional flows. Two explanations for the non-axisymmetry were given: Jiménez, Moffatt & Vasco (1996) showed that it could be induced by an external strain field; Rossi, Lingevitch & Bernoff (1997) demonstrated that it could be the result of a nonlinear perturbation of an axisymmetric vortex. In this paper, an asymptotic solution that describes both situations is provided.

The emergence of isolated coherent vortices is recognized as an important aspect of two-dimensional turbulence (e.g. McWilliams 1984). Several studies have been dedicated to the characterization of such structures. They have claimed that the selection of the vortex shape which seems to be mostly circular was the result of an 'axisymmetrization' process. This process was analysed by Melander, McWilliams & Zabusky (1987) for a class of elliptic vortices. They demonstrated that the vortex relaxes to an axisymmetric state on a time scale much shorter than the viscous

scale. Bernoff & Lingevitch (1994) analysed the same mechanism by considering the relaxation of a Lamb–Oseen vortex. They showed that the axisymmetrization was due to the shear-diffusion averaging mechanism of Lundgren's (1982) model: the non-axisymmetric perturbations are wound up into spiral structures due to the differential rotation of the vortex and then dissipated on an $O(Re^{1/3})$ time scale. Bassom & Gilbert (1998) recently considered the same issue in a non-viscous and linear framework. For a large class of regular vortices, they provided the asymptotic solution describing the asymmetrization process for large t. When the perturbations are large, their linear scenario does not necessarily apply. Indeed, Rossi *et al.* (1997) showed that a Lamb–Oseen vortex could relax to a tripole structure when perturbed by a large quadrupole perturbation. Such a structure as well as higher-order multipolar structures were also observed in rotating fluids where they may appear spontaneously under certain conditions. These strongly non-axisymmetric vortices have been the subject of numerous works (see for instance, Hopfinger & van Heijst 1993 and references therein). Apparently they are all composed of a vortex core surrounded by 2, 3 or more vortices of opposite sign.

Dritschel (1998) analysed the existence of non-axisymmetric vortices which still have a monopolar structure, i.e. for which there is a single centre of vortex motion. By considering a family of discontinuous vorticity profile including vortex patches, he numerically showed that an elliptically perturbed vortex could remain non-axisymmetric for a long time if the vortex has sufficiently steep edge gradients. However, the role of nonlinearity is not clear in this case as the linear axisymmetrization process of Bassom & Gilbert (1998) only applies to continuous vorticity profiles.

Non-axisymmetric structures in the charge density were also observed in magnetically confined columns of electrons (Driscoll & Fine 1990). These structures should correspond to non-axisymmetric vortices thanks to a known isomorphism between the 2D Euler equations and the 2D drift-Poisson equations describing this medium (Levy 1965). In that framework, the axisymmetrization process was studied by Mitchell & Driscoll (1994). Stability results were also obtained by Briggs, Daugherty & Levy (1970) and more recently by Schecter *et al.* (1998). They will be re-examined in the context of two-dimensional vortex flow in the last section of this paper.

Non-axisymmetry may also be due to an external strain field. Indeed, it is well-known that a vortex patch becomes elliptical when subject to an external strain field (Moore & Saffman 1971). This is also true for a continuous vorticity profile as shown by Ting & Tung (1965) and Jiménez *et al.* (1996). Based on Moffatt, Kida & Ohkitani's (1994) results for stretched vortices, Jiménez *et al.* (1996) demonstrated that a diffusing vortex could survive a very long time in an external strain field if the Reynolds number based on the vortex circulation was sufficiently large. In this limit, they computed the first elliptic correction to the vortex induced by a stationary external strain field. They applied their results to vortices of decaying two-dimensional turbulence and showed that quantities such as the eccentricity and the orientation angle of the elliptical streamlines in the vortex cores could be qualitatively understood by their model for a majority of them. Ting & Tung (1965) gave the equations for the linear correction to a Lamb vortex induced by a general external field. Lingevitch & Bernoff (1995) analysed the Reynolds-number dependence of the vorticity correction. When the external field is a rotating strain field, they found that the amplitude of the vorticity correction could become $O(Re^{1/3})$ for resonant angular frequencies. They also obtained the variation of the vorticity maximum with respect to the angular frequency of the strain field.

The paper is organized as follows. In § 2, the basic equations governing the non-axisymmetric corrections to a vortex subject to an external multipolar strain field rotating around the vortex axis are given. As in Jiménez *et al.* (1996), the framework is for large Reynolds number and small perturbation amplitude. Although it extends Jiménez *et al.*'s (1996) analysis, most equations were already given in Ting & Tung (1965) and Lingevitch & Bernoff (1995). The extension to a rotating strain field is needed in practice as the external strain field of a given vortex is generally created by other vortices rotating around it due to their mutual interactions. The general case of a multipolar strain field is considered in order to also describe flows which exhibit a fold symmetry of higher order. The basic equations are solved for a Gaussian vorticity profile in § 3.1 when the angular frequency of the external field is not in the range of the angular velocities of the vortex and in § 3.2 when it is. In this second case, the analysis turns out to be different due to the presence of a critical layer around the radial coordinate where the local angular velocity equals the frequency of the strain. The resolution of this singularity by the introduction of nonlinearity or viscosity is shown to govern the entire solution. The parameter which controls the nature of the critical layer is the parameter $h = 1/(Re\,\varepsilon^{3/2})$, where ε is the amplitude of the non-axisymmetric correction and Re the Reynolds number based on the circulation of the vortex (Haberman 1972). Numerous properties of the solutions as h varies are presented in § 3.2. In particular, the variations of the vorticity correction maximum are computed and compared in the viscous regime to the numerical results by Lingevitch & Bernoff (1995).

The nonlinear regime ($h \ll 1$) turns out to be particularly interesting as it may provide for a distinguished frequency a non-axisymmetric vortex for which the external strain field can be turned off. In other words, the external field is no longer needed to maintain the non-axisymmetry of the vortex in that case. Section 4 focuses on these non-axisymmetric vortices without external field. Their characteristic properties are computed for a family of vortex profiles ranging from Gaussian to top-hat. In § 5, the results are compared to Rossi *et al.*'s (1997), and Dritschel's (1998) computations. They are discussed and connected to recent results obtained for confined electron columns in § 6. In that section, transient effects are also briefly considered.

2. Slightly non-axisymmetric vortices

Consider an axisymmetric two-dimensional vortex of maximum vorticity ω_{max} and radius a perturbed by a non-axisymmetric disturbance and non-dimensionalize all the quantities using a and ω_{max}. The streamfunction Ψ and vorticity ω of the resulting field satisfy the two-dimensional incompressible Navier–Stokes equations

$$\frac{\partial \omega}{\partial t} + J[\omega, \Psi] = \frac{1}{Re}\Delta\omega, \tag{2.1}$$

$$\omega = -\Delta\Psi, \tag{2.2}$$

where the Jacobian operator $J[f, g]$ is defined in polar coordinates (r, θ) by

$$J[f, g] = \frac{1}{r}\left(\frac{\partial f}{\partial r}\frac{\partial g}{\partial \theta} - \frac{\partial g}{\partial r}\frac{\partial f}{\partial \theta}\right),$$

and the Reynolds number Re by $Re = \omega_{max}a^2/\nu$ where ν is the kinematic viscosity.

Assuming a small disturbance, one can write

$$\Psi = \mathrm{Re}\,\{\Psi_0(r) + \varepsilon\Psi_1(r, \theta, t) + O(\varepsilon^2)\}, \tag{2.3}$$

where Re denotes the real part, $\Psi_0(r)$ and $\Psi_1(r,\theta,t)$ are the streamfunctions of the axisymmetric vortex and the disturbance, respectively, and ε a small parameter which measures the size of the disturbance in the vortex core. This parameter is unambiguously defined by equations (2.4) and (2.9) given below.

As long as one neglects the viscous diffusion of the vortex and strong nonlinear effects, the disturbance can be decomposed into normal modes

$$\Psi_1(r,\theta,t) = \Phi_1(r)\mathrm{e}^{\mathrm{i}n(\theta-wt)}, \tag{2.4}$$

where n and w are the azimuthal wavenumber and the angular frequency, respectively. Under these conditions which require both $1/Re$ and ε to be small, the function Φ_1 satisfies, at leading order, the following ordinary differential equation:

$$(\Omega_0(r) - w)\Delta_n\Phi_1 = \frac{\omega_0'(r)}{r}\Phi_1, \tag{2.5}$$

where the prime denotes differentiation with respect to the argument, the angular velocity Ω_0 and the vorticity ω_0 of the underlying axisymmetric vortex are

$$\Omega_0 = -\frac{1}{r}\frac{\mathrm{d}\Psi_0}{\mathrm{d}r}, \tag{2.6}$$

$$\omega_0 = -\Delta_0\Psi_0, \tag{2.7}$$

and

$$\Delta_n = \frac{\mathrm{d}^2}{\mathrm{d}r^2} + \frac{1}{r}\frac{\mathrm{d}}{\mathrm{d}r} - \frac{n^2}{r^2}. \tag{2.8}$$

In this paper, we consider localized vortices which are stable with respect to the two-dimensional Rayleigh instability. This means that the vorticity is monotonically decreasing, rapidly goes to zero far from the vortex axis, and reaches its maximum in the vortex centre $r = 0$. For this category of vortices, the non-dimensionalized angular velocity $\Omega_0(r)$ varies from $\frac{1}{2}$ to 0 as r goes from 0 to $+\infty$. Here, we mostly focus on vorticity profiles ranging from Gaussian to top-hat but other profiles can be similarly considered.

Except for $w \neq \Omega_0(0) = 1/2$, the two possible behaviours near $r = 0$ of solutions to (2.5) are r^n and r^{-n}. Discarding the singular behaviour, one can then impose (for any $w \neq \Omega_0(0)$)

$$\Phi_1 \sim r^n \quad \text{as } r \to 0. \tag{2.9}$$

This condition fixes the normalization of the amplitude of the non-axisymmetric correction and defines in an unambiguous way the parameter ε. Moreover, condition (2.9) also selects a single solution to equation (2.5). The behaviour of that solution near infinity is easily shown to be

$$\Phi_1 \sim s_n r^n + \frac{c_n}{r^n} \quad \text{as } r \to \infty, \tag{2.10}$$

where s_n and c_n are two constants which depend on w and on the way eventual singularities of the equation are resolved. When s_n is non-zero, the total streamfunction Ψ does not vanish for large r and behaves as

$$\Psi \sim \varepsilon|s_n|r^n \cos\left[n(\theta - wt) + \arg(s_n)\right] \quad \text{as } r \to \infty. \tag{2.11}$$

This expression represents the external field which is needed to maintain the non-axisymmetric correction Φ_1 in (2.3) with the normalization (2.9). It is a multipolar strain field with an n-fold symmetry rotating at the angular frequency w.

If $s_n = 0$, the strain field is generated by the vortex itself as no external field is present anymore. In that case, Φ_1 represents an eigenmode of the vortex and expression (2.3) is then the first-order approximation of the streamfunction of a non-axisymmetric vortex solution in a strain-free environment. Note also that if equation (2.5) were valid everywhere for such an eigenmode, the mixing hypothesis of Bassom & Gilbert (1998) would not apply as there would exist linear inviscid non-axisymmetric perturbations which do not decay. We shall see below that this does not occur. However, as equation (2.5) naturally develops singularities, the vanishing of s_n will be shown to be possible if the singularities are smoothed by nonlinearities. The properties of such nonlinear perturbations are analysed in detail in § 4. The resulting non-axisymmetric vortices are compared to the numerical solution of Rossi *et al.* (1997) in § 5.

3. Vortices in a rotating multipolar strain field

The linear problem (2.5), (2.9), (2.10) is analogous to the one obtained in Moffatt *et al.* (1994) and Jiménez *et al.* (1996) for the stationary elliptic correction of a Gaussian vortex. In particular, equation (2.25) in Moffatt *et al.* (1994) corresponds to (2.5) for the particular values $n = 2$, $w = 0$ and the vorticity profile

$$\omega_0(r) = G(r) \equiv \exp(-r^2). \tag{3.1}$$

Note however that a different normalization has been chosen: the amplitude of Φ_1 is fixed in the vortex core by the condition (2.9), hence the unknown parameter is here $s_n(w)$ and not the strain rate in the vortex core as in Moffatt *et al.* (1994) or Jiménez *et al.* (1996). As explained above, this choice which allows $s_n = 0$ has been made in order to treat in the same framework non-axisymmetric vortices without external strain field (see § 4).

Lingevitch & Bernoff (1995) also considered a problem similar to (2.5), (2.9), (2.10) but they kept the viscous terms in the equation for the non-axisymmetric correction.

The resolution of (2.5), (2.9) and (2.10) crucially depends on the value of w with respect to the range of Ω_0. If w is in the range of Ω_0, i.e. $\min(\Omega_0) < w < \max(\Omega_0)$, there exists a critical point r_c defined by $\Omega_0(r_c) = w$ where solutions of (2.5) (or their derivatives) may exhibit a singularity. In other words, the solution of (2.5) prescribed by (2.9) may become singular at r_c. The resolution of this singularity would require the introduction of higher-order effects such as viscosity or nonlinearity. Before treating this case which will turn out to be the most interesting, let us first consider the no-critical-layer case.

3.1. *No critical layer*

The configurations without a critical layer correspond to frequencies satisfying

$$w < \min(\Omega_0) = 0 \quad \text{or} \quad w > \max(\Omega_0) = 1/2.$$

For these frequencies, the integration of (2.5) with condition (2.9) at zero is possible from 0 to ∞ and provides a function Φ_1 differential everywhere. The parameter $s_n(w) = \lim_{r\to\infty}(\Phi_1/r^n)$ is then perfectly defined in a linear non-viscous framework. This parameter gives both the strength $|s_n|$ of the external field and its phase shift $\arg(s_n)$ with respect to the orientation of the perturbation in the vortex core. Without a critical layer, s_n is real positive, so there is no modification of the orientation of the perturbation in the vortex core with respect to the external field. In figure 1 is represented the variation of $s_n(w)$ with respect to w for the Gaussian vorticity profile (3.1) and $n = 2, 3, 4, 5$. For this profile, the frequency interval $(0, 0.5)$ has been excluded

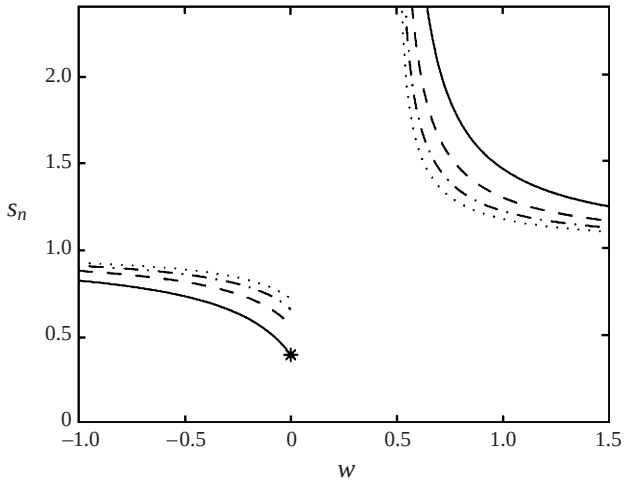

FIGURE 1. Coefficient s_n versus the angular frequency w for a Gaussian vorticity profile. Solid line: $n = 2$; dashed line: $n = 3$; dash-dotted line: $n = 4$; dotted line: $n = 5$. The star indicates the value given in Jiménez *et al.* (1996).

as it corresponds to configurations with a critical layer. As in Jiménez *et al.* (1996), for $n = 2$, the streamlines of the resulting vortex are elliptical with major axis oriented at 45° with respect to the strain. Moreover, the eccentricity of the streamline in the vortex centre is given by $1/s_2$ when the external strain field is normalized at infinity. Figure 1 shows that, when no critical layers are present, the vortex eccentricity is maximum for $w = 0$: the effect of rotation of the strain field is then to diminish the strain strength in the vortex core. Note also that the non-axisymmetric distortion is stronger in the vortex core than outside for anticyclonic vortices ($s_n < 1$ if $w < \min(\Omega_0) = 0$) while it is the opposite for strongly cyclonic vortices ($s_n > 1$ if $w > \max(\Omega_0) = 1/2$).

For the critical value $w = 1/2 = \Omega_0(0)$, condition (2.9) does not apply. The adequate behaviour of Φ_1 near zero is in fact $r^{\sqrt{n^2+8}}$ and not r^n (Bassom & Gilbert 1998). Enforcing condition (2.9) close to $w = 1/2$ would lead to very large values of s_n which could explain the divergence of s_n observed in figure 1 near $w = 1/2$. Note however that since $r^{\sqrt{n^2+8}}$ is in general not infinitely differentiable near $r = 0$, an inner solution involving other effects such as viscosity, nonlinearity or non-stationarity, is *a priori* needed near the vortex centre to smooth the irregularity. Such an inner solution has been calculated by Bassom & Gilbert (1998) in the limit of large time when time-dependent effects are dominant.

It is also worth mentioning that the results presented in figure 1 are qualitatively the same for all n. We shall see below that this is no longer the case when there are critical layer singularities.

3.2. *Critical layer analysis*

Critical layers are well-known in the parallel shear flow framework and refer to regions close to the (critical) points where the basic flow velocity equals the phase velocity of the perturbation. They have been the subject of numerous works since the fifties and are now recognized to play an essential role in shear flow transition (see Maslowe 1986, and references therein). Here the critical points are the radial positions r_c where the angular velocity of the vortex equals the angular frequency of the perturbation, that is where $\Omega_0(r_c) = w$. The critical layers around these points are

the same as in the parallel flow case. We shall assume that the critical layers are in equilibrium, such that classical results from Benney & Bergeron (1969), Haberman (1972), Brown & Stewartson (1978) and Smith & Bodonyi (1982) can be used. A brief account of time-dependent effects is given in the discussion.

If $\Omega_0(r_c) = w$, starting to integrate equation (2.5) on the real axis from $r = 0$ with condition (2.9) ultimately leads to a solution which exhibits at the critical point r_c for $r < r_c$ a weak singularity of the form

$$\Phi_1(r) \sim \alpha + \beta(r - r_c) + \alpha\kappa_c(r - r_c)\ln(r_c - r) \quad \text{as } r \to r_c^-, \tag{3.2}$$

where α and β are real constants and $\kappa_c = \omega_0'(r_c)/(r_c\Omega_0'(r_c))$. This weak singularity of the streamfunction is associated with a true singularity of the vorticity field which is usually solved in a 'critical layer' by considering higher-order terms such as viscous or nonlinear terms (Lin 1955; Benney & Bergeron 1969; Haberman 1972). The main result, as far as we are concerned, is that an azimuthal velocity jump is created across the critical layer such that the amplitude Φ_1 of the streamfunction (2.4) has an expansion for $r > r_c$ of the form

$$\Phi_1(r) \sim \alpha + \beta(r - r_c) + \alpha\kappa_c(r - r_c)[\ln|r - r_c| + \mathrm{i}\chi] \quad \text{as } r \to r_c^+. \tag{3.3}$$

The value of χ depends on the nature of the critical layer, that is whether nonlinearity or viscosity dominates near $r = r_c$. Lin (1955) showed that $\chi = -\pi$ if $\mathrm{sgn}(n\Omega_0'(r_c)) < 0$ ($\chi = +\pi$ if $\mathrm{sgn}(n\Omega_0'(r_c)) > 0$) when the critical layer is viscous. Benney & Bergeron (1969) obtained $\chi = 0$ for a purely nonlinear critical layer. Haberman (1972) considered both effects simultaneously and proved that χ varies continuously from $-\pi$ to 0 when non-linearity is progressively increased. Moreover, he showed that χ depends on a single parameter† h given by

$$h \equiv \frac{h_c}{\varepsilon^{3/2}Re}\,, \tag{3.4}$$

where the coefficient h_c is here

$$h_c = \frac{|\Omega_0'(r_c)|^{1/2}}{n}\left|\frac{r_c}{\Phi_1(r_c)}\right|^{3/2}. \tag{3.5}$$

The algebraic manipulations leading to (3.4) and (3.5) are given in the Appendix, as well as the curve $\chi(h)$ obtained by Haberman (1972) and Smith & Bodonyi (1982). With this definition of h, the critical layer is then viscous if $h \gg 1$, and purely nonlinear if $h \ll 1$.

Once h is computed, $\chi(h)$ is known from figure 14 in the Appendix, so that equation (2.5) can be integrated from r_c to $+\infty$ with condition (3.3). Near infinity, the solution behaves according to (2.10). The form of expansion (3.3) guarantees that s_n can be written as

$$s_n(w, h) = s_n^{NL}(w) - \mathrm{i}\frac{\chi(h)}{\pi}s_{n,i}^{V}(w), \tag{3.6}$$

where s_n^{NL} and $s_{n,i}^{V}$ are two real functions. These functions are the limit values for large r of $f(r)/r^n$ and $g(r)/r^n$, respectively, where f and g are solutions of (2.5) prescribed

† This parameter is here designated by the letter h instead of λ as usually done in critical layers works (see Maslowe 1986) because λ often refers to the non-axisymmetric part of the strain in the vortex literature (see e.g. Moffatt *et al.* 1994). Moreover, this parameter was sometimes called Haberman parameter (Goldstein & Hultgren 1988), so 'h' seems adequate.

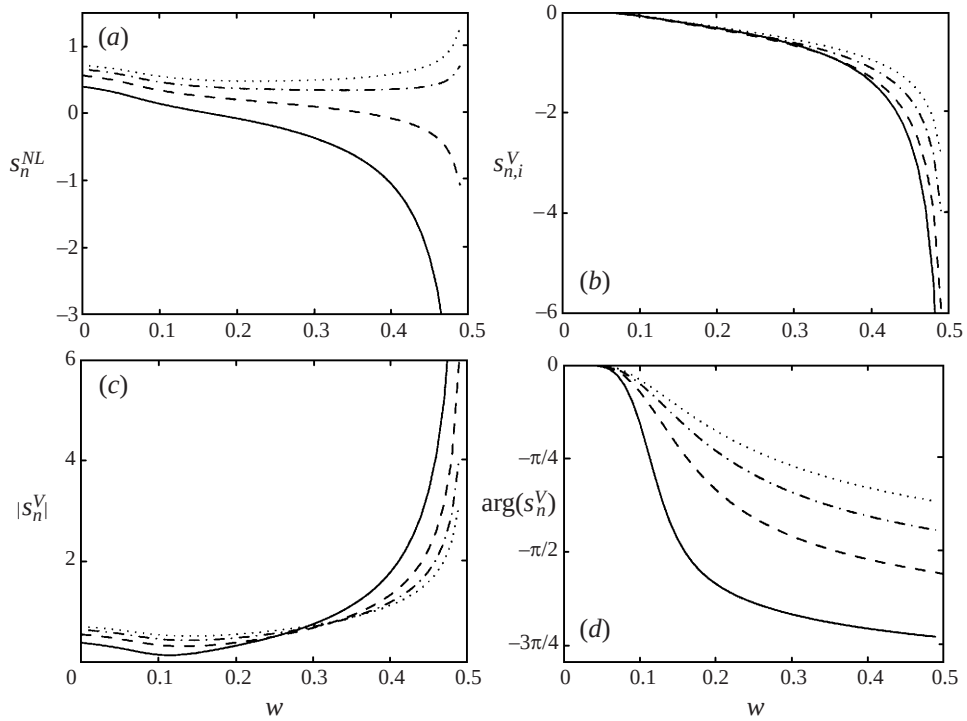

FIGURE 2. Variation of s_n^V with respect to the angular frequency w for a Gaussian vortex. Solid line: $n = 2$; dashed line: $n = 3$; dash-dotted line: $n = 4$; dotted line: $n = 5$. (*a*) Real part (s_n^{NL}); (*b*) imaginary part ($s_{n,i}^V$); (*c*) modulus ($|s_n^V| = [(s_n^{NL})^2 + (s_{n,i}^V)^2]^{1/2}$), (*d*) phase ($\arg(s_n^V) = \arctan(s_{n,i}^V/s_n^{NL})$). Figures (*c*) and (*d*) provide the strength and phase shift of the external strain field in the viscous critical layer regime.

by the following expansions near r_c^+:

$$f(r) \sim \alpha + \beta(r - r_c) + \alpha\kappa_c(r - r_c)\ln|r - r_c| \quad \text{as } r \to r_c^+, \tag{3.7}$$

and

$$g(r) \sim \frac{\alpha\kappa_c}{\pi}(r - r_c) \quad \text{as } r \to r_c^+. \tag{3.8}$$

It immediately follows that $s_n = s_n^{NL}$ for a purely nonlinear critical layer ($\chi = 0$), and $s_n = s_n^V = s_n^{NL} + is_{n,i}^V$ for a purely viscous critical layer ($\chi = -\pi$).

Results for the Gaussian vorticity profile (3.1) are now discussed. The variations of s_n^{NL} and $s_{n,i}^V$ with respect to w are displayed on figures 2(*a*) and 2(*b*) for $n = 2, 3, 4, 5$. These figures complete figure 1. They provide s_n for any value of h thanks to expression (3.6) and figure 14 for $\chi(h)$. The first important point to note is that s_n is in general complex, which means that both the orientation and the strength of the non-axisymmetric distortion varies with respect to the radial coordinate. The change of orientation in the vortex core between critical layer and no critical layer cases is measured by the phase of s_n which reaches its maximum for the viscous case ($\chi = -\pi$). The variation of this maximum with respect to w is shown on figure 2(*d*). The corresponding modulus of s_n is displayed on figure 2(*c*). For $n = 2$, figure 2(*d*) implies that the elliptical streamlines near the centre no longer have a major axis oriented at 45° with respect to the external strain but that there is an additional angular shift $\phi_2 = -\arg(s_2)/2$. This additional shift is maximum for viscous critical

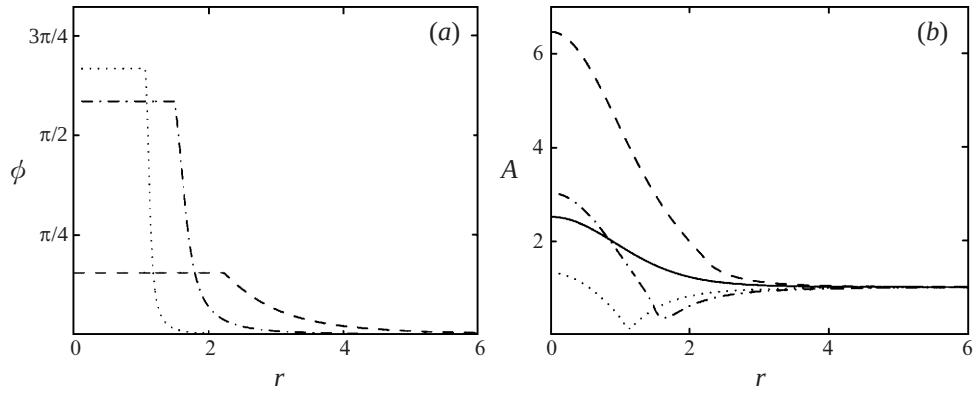

FIGURE 3. Phase ϕ (a) and amplitude A (b) of the elliptic distortion (as defined in (3.9)) for a Gaussian vorticity profile and a viscous critical layer ($h \gg 1$). Solid line: $w = 0$; dashed line: $w = 0.1$; dash-dotted line: $w = 0.2$; dotted line: $w = 0.3$.

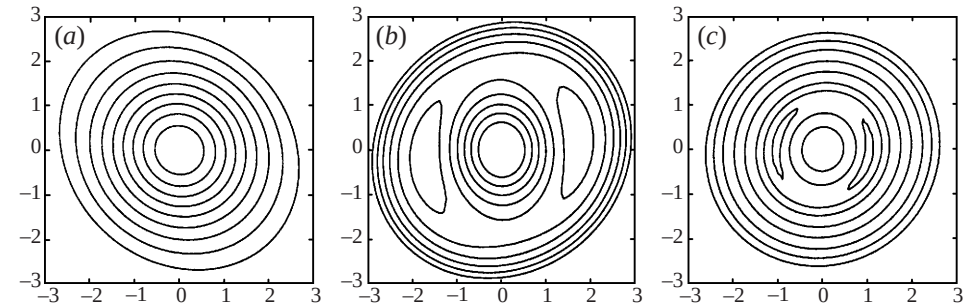

FIGURE 4. Streamlines of the perturbed Gaussian vortex in the frame co-rotating with the external strain field with a viscous critical layer. ($\varepsilon = 0.005$) (a) $w = 0$, (b) $w = 0.15$, (c) $w = 0.3$.

layers and grows with w up to $|\phi_2|_{\max} \approx 1.15$. This effect can also be seen on figures 3 and 4. On figures 3(a) and 3(b) are represented variations of the phase and amplitude of the non-axisymmetric distortions as a function of the radial coordinate r for different frequencies where amplitude A and phase ϕ are defined from Φ_1 by

$$\Phi_1 = s_2 r^2 A(r) \mathrm{e}^{\mathrm{i}\phi(r)}. \tag{3.9}$$

On figure 4 are displayed the streamlines of the elliptically perturbed Gaussian vortex in a frame co-rotating with the external strain field for three different values of the frequency and for fixed ε. One clearly sees that from left to right the orientation of the elliptic streamlines in the vortex core rotates clockwise. Two regions of recirculation located outside the vortex axis are also present in figures 4(b) and 4(c). They are associated with the critical layer. Their position moves towards the vortex centre as the frequency increases, as expected from the displacement of the critical point r_c towards the centre.

In figure 5 is plotted the amplitude A of the correction Φ_1 as defined in (3.9) when the critical layer is purely nonlinear ($\chi = 0$) for the same values of w as in figure 3(b). The important differences between figures 3(b) and 5 demonstrate that the nature of the critical layer has a strong influence on the structure of the non-axisymmetric distortion everywhere.

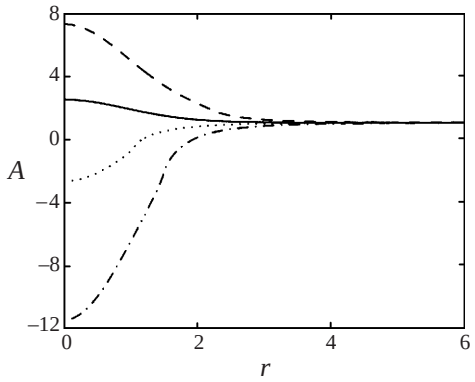

FIGURE 5. Amplitude A of the elliptic distortion (as defined in (3.9)) for a Gaussian vorticity profile and a nonlinear critical layer ($h \ll 1$). Solid line: $w = 0$; dashed line: $w = 0.1$; dash-dotted line: $w = 0.2$; dotted line: $w = 0.3$.

An even more important consequence is that the parameter $|s_n|$ may vanish or not according to the nature of the critical layer as w varies. For a Gaussian vorticity profile, figure 2(a) gives the value of $|s_n|$ when the critical layer is nonlinear. It can be seen that both s_2 and s_3 vanish for $w \approx 0.160$ and $w \approx 0.358$ respectively, while s_4 and s_5 never vanish. When viscous effects are present in the critical layer, s_n has an additional imaginary part, proportional to $s^V_{n,i}$ given in figure 2(b), which precludes the vanishing of $|s_n|$. This property is not limited to Gaussian vortices. In the next section, we shall see for a family of vortex profiles ranging from Gaussian to top-hat, that $|s_n|$ does not vanish in the viscous critical layer regime.

As mentioned in § 2, $|s_n|$ measures the strength of the external field needed to maintain a non-axisymmetric distortion normalized in the vortex centre. Its inverse $1/|s_n|$ then indicates the strength of the distortion in the vortex centre in a normalized external field. If an external strain field is imposed at a frequency such that $s_n = 0$ the vortex cannot reach the equilibrium state described here, as it would imply the blow up of the non-axisymmetric distortion in the vortex centre. This means either that another analysis should be developed in the vortex centre in order to describe the strong deformation of the vortex core that this blow up would imply, or that other effects such as time-dependence could become important. One could indeed imagine that inertial waves could be generated in the critical layer such that the strain rate does not blow up in the vortex centre. This picture is attractive because it may qualitatively explain the ejection and spiral wind up of vorticity often observed in vortex interactions before merging (Dritschel 1995; Driscoll & Fine 1990).

Whereas the distortion streamfunction can be plotted without resolving the critical layer, the determination of the vorticity requires the full resolution of the critical layer. It is indeed in the critical layer that the singularity of the outer solution is smoothed out. As a consequence, it is also in the critical layer that the largest vorticity corrections are obtained. The form of the vorticity field in the critical layer is given in the Appendix (see expression (A 18)). It is also shown that the maximum of the non-axisymmetric vorticity correction reads

$$\omega^{NA}_{max}(h, w, n) = F_n(w)M(h)\sqrt{\varepsilon}, \tag{3.10}$$

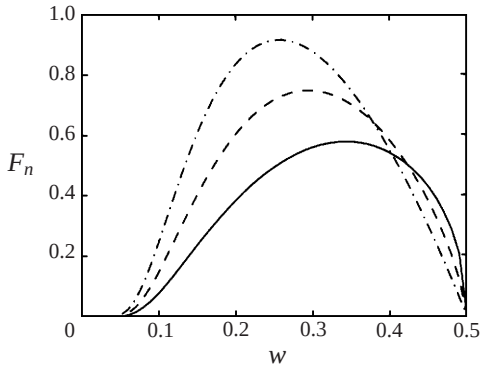

FIGURE 6. Non-axisymmetric vorticity maximum for a correction normalized in the vortex centre: variation of the amplitude factor F_n versus the angular frequency w. Solid line: $n = 2$; dashed line: $n = 3$; dash-dotted line: $n = 4$.

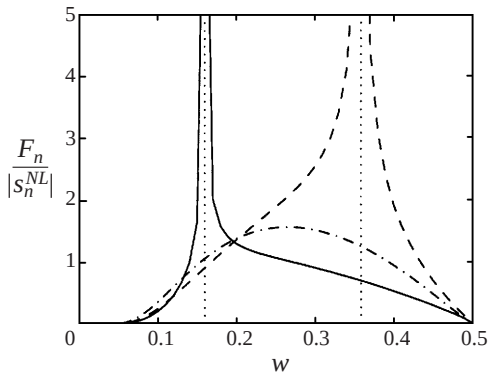

FIGURE 7. Non-axisymmetric vorticity maximum of the correction generated by a normalized external field in the nonlinear critical layer regime: variation of the amplitude factor $F_n/|s_n^{NL}|$ versus the angular frequency w of the external field. Solid line: $n = 2$; dashed line: $n = 3$; dash-dotted line: $n = 4$.

where the function $M(h)$ is defined by (A 22) and

$$F_n(w) = |\omega'_{0_c}| \left| \frac{\Phi_{1_c}}{r_c \Omega'_{0_c}} \right|^{1/2}, \tag{3.11}$$

where the subscript c indicates values taken at r_c. This expression demonstrates that, for all $h = O(1)$, the maximum of non-axisymmetric vorticity is $O(\sqrt{\varepsilon})$ whereas the amplitude of the streamfunction is $O(\varepsilon)$. Moreover, for any fixed h and ε, the non-axisymmetric vorticity maximum varies according to the same function $F_n(w)$, which is plotted in figure 6. These variations are for a distortion normalized in the vortex centre. When the distortion is normalized at infinity, for instance, by using a fixed external field $\Psi_n = \varepsilon r^n \cos[n(\theta - wt)]$, the vorticity maximum ω_{max}^{NA} is divided by $|s_n|$. Figure 7 shows the variation of the vorticity maximum $F_n/|s_n^{NL}|$ for such a case in the nonlinear critical layer regime ($h \ll 1$). The blow up of the vorticity maximum is due to the vanishing of $|s_n^{NL}|$.

In the viscous critical layer regime ($h \gg 1$), expression (3.10) for the vorticity

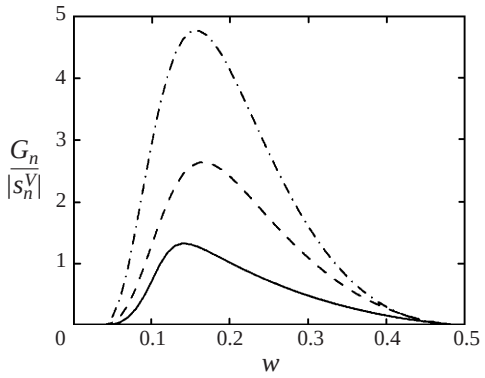

FIGURE 8. Vorticity maximum of the correction generated by a normalized external field in the viscous linear regime: variation of the amplitude factor $G_n/|s_n^V|$ versus the angular frequency w of the external field. Solid line: $n = 2$; dashed line: $n = 3$; dash-dotted line: $n = 4$.

correction maximum is replaced by (see expression (A 23))

$$\omega_{max}^{NA} = G_n(w) M_v Re^{1/3} \varepsilon, \tag{3.12}$$

where M_v is a numerical constant defined in the Appendix and

$$G_n(w) = |\omega_{0_c}'| \frac{|\Phi_{1_c}|}{|r_c||\Omega_{0_c}'|^{2/3}} n^{1/3}. \tag{3.13}$$

In that regime, the vorticity correction is then $O(Re^{1/3})$ larger than the streamfunction. This was already pointed out by Lingevitch & Bernoff (1995) who numerically calculated the vorticity correction generated by a rotating strain field in the linear viscous regime. In figure 8 is plotted $G_n/|s_n^V|$ which describes the variation of the vorticity correction maximum for a normalized external field and a fixed Reynolds number. The curve for $n = 2$ is in very good agreement with the numerical results of Lingevitch & Bernoff (1995). In particular, the angular frequency $w_{max} \approx 0.1412$ which maximizes the vorticity response is within 0.1% the value obtained by Lingevitch & Bernoff (1995) for large Reynolds number simulations.

We have seen that solutions with $s_n = 0$ cannot exist with an external field. Nevertheless, these solutions are very interesting when no external field is present because they become very good candidates for non-axisymmetric vortices. In the next section, they are studied in more detail for a family of vorticity profiles ranging from Gaussian to top-hat.

4. Non-axisymmetric vortices without external strain field

This section focuses on the non-axisymmetric solution for which the external strain field is turned off ($s_n = 0$). The main goal is to analyse the effect of the vorticity profile on the characteristics of the non-axisymmetric distortion. In particular, we want to address the role of steep edge gradients in the existence of such solutions. For this purpose, we consider a family of vorticity profiles defined by

$$\left.\begin{aligned} \omega_0(r) &= 1, & r < a, \\ \omega_0(r) &= \exp\left(-\frac{(r-a)^2}{(1-a)^2}\right), & r \geqslant a, \end{aligned}\right\} \tag{4.1}$$

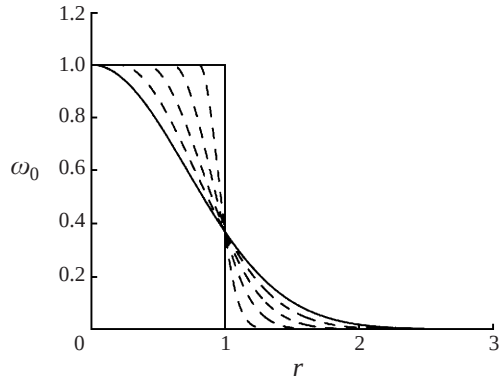

FIGURE 9. Vorticity profile (4.1) for $a = 0 : 0.2 : 1$. The Gaussian profile corresponds to $a = 0$.

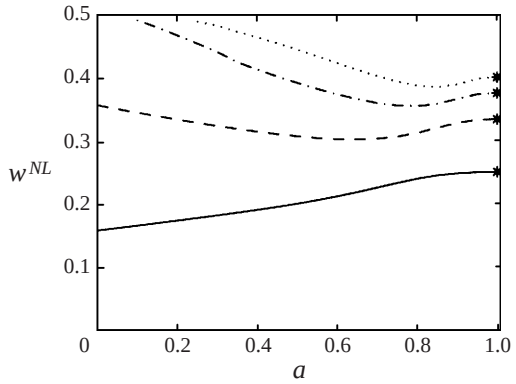

FIGURE 10. Angular frequency w^{NL} of the eigenmode as a function of the vorticity profile parameter a. Solid line: $n = 2$; dashed line: $n = 3$; dash-dotted line: $n = 4$; dotted line: $n = 5$. The stars are the linear prediction for Rankine vortex (equation (4.4)).

with $0 \leqslant a \leqslant 1$, which describe vortices ranging from the Gaussian vortex ($a = 0$) to the Rankine vortex ($a = 1$) (see figure 9). Note that, except for $a = 1$, these vortices are not compact. As discussed in § 5 in relation to the results of Dritschel (1998), this property makes them significantly different from compact vortices.

Based on the results of the previous section, non-axisymmetric solutions without external strain field are expected to exist only if they exhibit a nonlinear critical layer. In such a case the non-axisymmetric distortion is at leading order (see the Appendix for more details)

$$\Psi_1 = \varepsilon \Phi_1 \cos\left[n(\theta - wt)\right], \tag{4.2}$$

where Φ_1 satisfies equation (2.5) on the intervals $(0, r_c^-)$ and $(r_c^+, +\infty)$ with the boundary conditions

$$\Phi_1(r) \sim r^n \quad \text{as } r \to 0\ , \tag{4.3a}$$

$$\Phi_1(r) \sim \alpha + \beta(r - r_c) + \alpha\kappa_c(r - r_c)\ln|r - r_c| \quad \text{as } r \to r_c^-\ , \tag{4.3b}$$

$$\Phi_1(r) \sim \alpha + \beta(r - r_c) + \alpha\kappa_c(r - r_c)\ln|r - r_c| \quad \text{as } r \to r_c^+\ , \tag{4.3c}$$

$$\Phi_1(r) \sim Cr^{-n} \quad \text{as } r \to \infty\ , \tag{4.3d}$$

where $\alpha = \Phi_1(r_c)$, β and C are real numerical constants. For each a and n, integration

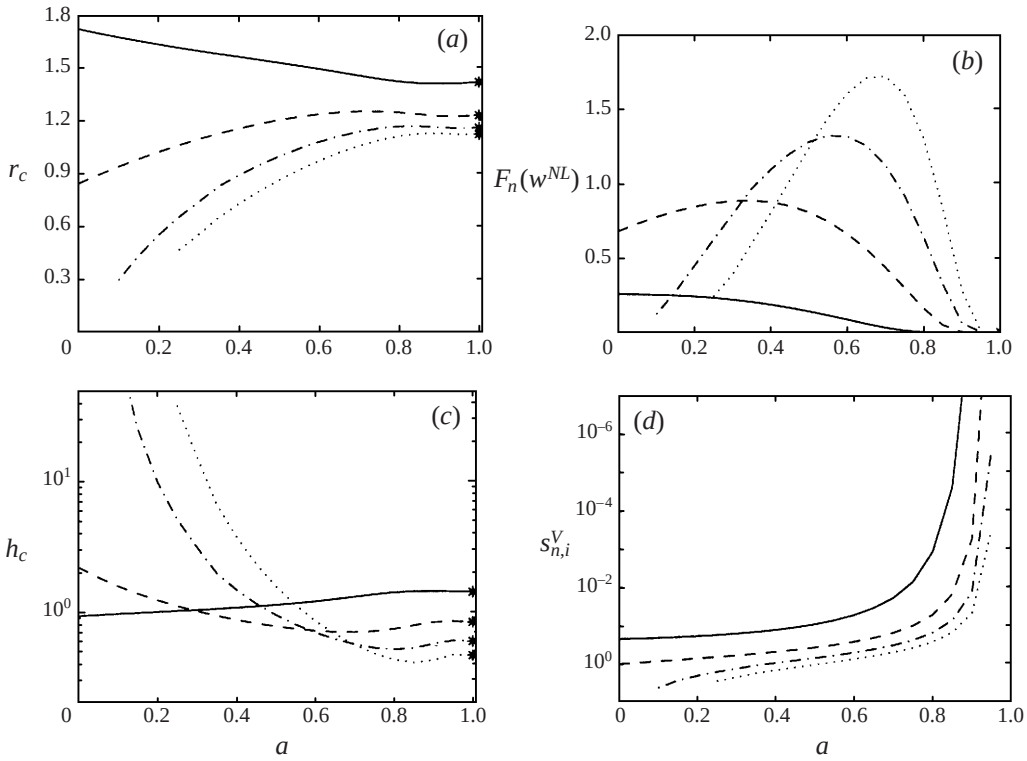

FIGURE 11. Characteristics of the nonlinear non-axisymmetric solution as a function of the vorticity profile parameter a. Solid line: $n = 2$; dashed line: $n = 3$; dash-dotted line: $n = 4$; dotted line: $n = 5$. The stars are the linear prediction for Rankine vortex. (a) Critical point r_c; (b) amplitude factor F_n appearing in the expression (4.5) of the vorticity jump across the critical layer and in the expression (3.10) of the vorticity correction maximum; (c) local Haberman parameter h_c (expression (3.5)); (d) strength $s^V_{n,i}$ of the external strain needed to maintain a non-axisymmetric solution at the nonlinear eigenfrequency in the viscous critical layer regime.

of (2.5) with these conditions leads to an eigenvalue problem for the angular frequency w. The results of the computation are presented on figure 10. It is seen that for $n = 2$ and $n = 3$ the angular frequency w^{NL} varies only slightly with a. For $n = 4, 5$ and larger, there exists a critical parameter a_c below which there is no eigenfrequency. This critical parameter increases with n and tends to 1 as n goes to infinity (not shown). For $n \geqslant 4$, a_c always corresponds to the case where the angular frequency reaches the maximum angular velocity of the vortex (here $1/2$), that is the upper bound of the frequency interval for which a critical layer exists. For each n, it is also seen that the angular frequency tends as $a \to 1$ to the linear prediction (e.g. Saffman 1992):

$$w_n = \frac{1}{2}\left(1 - \frac{1}{n}\right). \tag{4.4}$$

Other characteristic quantities of the eigenmodes are given in figure 11. The critical position r_c where the angular velocity Ω_0 equals the eigenfrequency w^{NL} is shown on figure 11(a). Its variation with respect to a and n reflects that of w^{NL}: r_c increases when w^{NL} decreases as expected from the decreasing behaviour of Ω_0. At r_c, the streamfunction of the eigenmode exhibits a vertical tangent. If the critical layer is

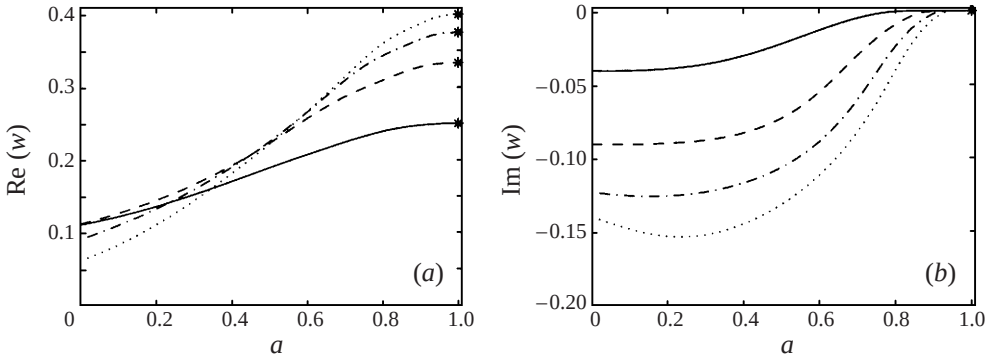

FIGURE 12. Linear eigenfrequency versus a. (a) Real part; (b) imaginary part (damping rate). The stars are the linear predictions for Rankine vortex (equation (4.4)).

in equilibrium as assumed, an axisymmetric vorticity jump is also created across the critical layer which has the form $\varepsilon^{1/2}\delta\omega$ at leading order. The expression for this jump is (see Appendix)

$$\delta\omega = 2CF_n(w^{NL}), \tag{4.5}$$

where the function $F_n(w)$ is defined in (3.11) and $C \approx 1.3$. Comparing expressions (3.10) and (4.5) shows that the axisymmetric vorticity jump varies exactly as the maximum of the non-axisymmetric components of the vorticity correction. The variation of $F_n(\omega^{NL})$ with respect to a is plotted in figure 11(b). The vanishing of $F_n(\omega^{NL})$ for a close to 1 can be understood by the presence of the term ω'_{0_c} which goes to zero as $a \to 1$. This means that close to $a = 1$, the jump and vorticity correction are no longer $O(\sqrt{\varepsilon})$ but become $O(\varepsilon)$.

The quantity h_c represented in figure 11(c) is the local Haberman parameter defined in equation (3.5) which characterizes the nature of the critical layer. From an asymptotical point of view, the nonlinear critical layer regime, required for the existence of the eigenmode, applies as soon as $h \ll 1$, that is

$$\varepsilon^{3/2}Re \gg h_c. \tag{4.6}$$

Thus, h_c indicates the amplitude threshold of the nonlinear eigenmode (the parameter ε) for a given Reynolds number, or the minimum Reynolds number required for the non-axisymmetric vortex solution formed with the nonlinear eigenmode at a given amplitude ε to survive.

If condition (4.6) is not satisfied, the nonlinear eigenmode does not exist. This means that either an external field is needed to maintain the non-axisymmetric disturbance, or the latter does not survive and probably decays. The modulus of the parameter $s^V_{n,i}$ plotted in figure 11(d) is the strength of the external field that is required to maintain a non-axisymmetric perturbation with the same frequency but with a viscous critical layer. When both nonlinear and viscous effects are present in the critical layer, the external field strength is $|s_n| = |[\chi(h)/\pi]s^V_{n,i}|$ where $\chi(h)$ is obtained from figure 14. As $|\chi(h)/\pi| \approx 1$ as soon as $h > 5$, the viscous critical layer estimate given by figure 11(d) approximately applies for all $h > 5$, i.e. $\varepsilon^{3/2}Re < 0.2h_c$. Note also that for smaller h, or larger $\varepsilon^{3/2}Re$, the external field is always weaker since $|\chi(h)/\pi| < 1$.

If condition (4.6) is not met and no external strain is present, one expects the non-axisymmetric distortion to be damped. In such a case, the critical point moves in the complex plane and it becomes much more difficult to take into account nonlinear

effects. However, if one assumes that nonlinear effects are negligible, the damped rate can be obtained from equation (2.5) alone by integrating along a path in the complex plane that contours the critical point from above. This procedure is also possible when the critical point is on the real axis and is equivalent to assuming that the critical layer is purely viscous (see Lin 1955, for instance). The result of this procedure for the vorticity profiles (4.1) is displayed in figure 12 where the real part and imaginary parts of the viscous eigenfrequency are given as a function of a. Comparing these plots with those for the real nonlinear eigenfrequency (figure 10), one immediately sees that the gap between the real nonlinear eigenfrequency and the complex viscous eigenfrequency increases as either a decreases or n increases. For the Gaussian vortex ($a = 0$), the elliptic distortion has for instance a damping rate $w_i \approx -0.04$ and a frequency $w_r \approx 0.11$ which differs from the nonlinear frequency by approximately 45%. For the 3-fold symmetrical distortion, $w_i \approx -0.09$ and $w_r \approx 0.11$, so the frequency difference between viscous and nonlinear regimes reaches 227% in that case. As a goes to 1, nonlinear and viscous frequencies collide.

An estimate for the viscous damping rate is now obtained using the perturbation method of Briggs *et al.* (1970). For a close to 1, the frequency is approximately given by (4.4), so that the critical point is at leading order at the location $r_c = [n/(n-1)]^{1/2}$. If one multiplies equation (2.5) by the conjugate of Φ_1, integrates from 0 to ∞ and takes the imaginary part of the resulting equation, one gets

$$-\mathrm{i}\pi \frac{\omega_0'(r_c)|\Phi_1(r_c)|^2}{r_c \Omega_0'(r_c)} + \mathrm{i}w_i \int_0^\infty \frac{\omega_0'(r)|\Phi_1(r)|^2}{|\Omega_0(r) - w_r|^2}\mathrm{d}r = 0. \tag{4.7}$$

If both terms are evaluated using the solution for $a = 1$, i.e.

$$\begin{aligned} \Phi_1(r) &= r^n, \quad && r < 1, \\ \Phi_1(r) &= 1/r^n, && r \geqslant 1, \end{aligned}$$

one finally obtains

$$w_i = \pi \frac{\omega_0'(r_c)}{r_c^{2n-2}} (\tfrac{1}{2} - w_r)^2,$$

i.e.

$$w_i = \frac{\pi}{4n^2} \omega_0'(\sqrt{n/(n-1)}) \left(\frac{n-1}{n}\right)^{n-1}. \tag{4.8}$$

The connection between the damping rate and the vorticity gradient at the critical point is clearly seen in this expression. It confirms that the tendency for the nonlinear and viscous frequencies to collide when a goes to 1 is directly related to the vanishing of the vorticity gradient at the critical point.

Note that a similar analysis is also possible to get an estimate for the strength $s_{n,i}^V$ of the external strain illustrated in figure 11(d) as a goes to 1. It leads to the same result that $s_{n,i}^V$ is proportional to the vorticity gradient of the vortex at the critical point, so that $s_{n,i}^V$ decreases exponentially fast to zero as $a \to 1$.

5. Comparison with numerical evidence

In this section, the results are compared to the numerical solutions obtained by Rossi *et al.* (1997) and Dritschel (1998).

Rossi *et al.* (1997) numerically demonstrated the existence of a non-axisymmetric vortex solution by perturbing a Lamb vortex with a localized elliptic distortion. We argue that their solution could be the non-axisymmetric state described in § 4.

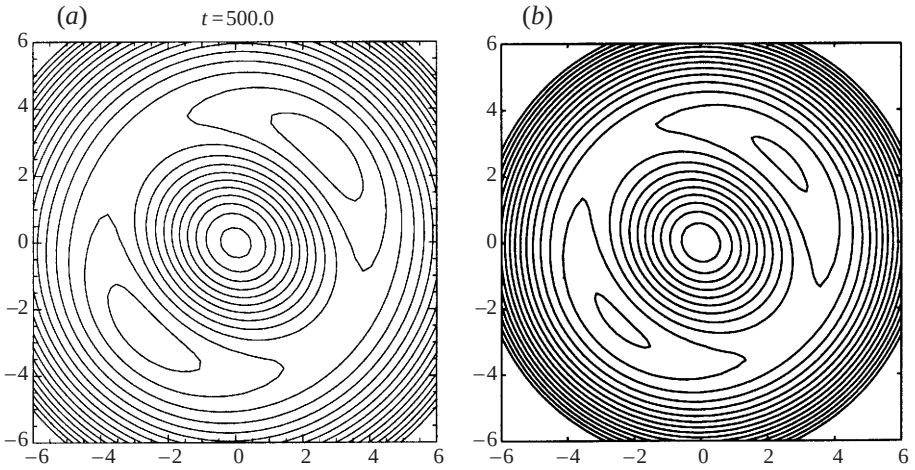

FIGURE 13. Streamlines in the co-rotating frame of the non-axisymmetric solution obtained from a Gaussian vortex. (*a*) Numerical solution (from Rossi *et al.* 1997), (*b*) asymptotic solution with $\varepsilon = 0.02$.

Figure 13(*a*) is taken from Rossi *et al.* (1997) and shows the streamlines of their vortex in a co-rotating frame for $Re = 10^4$. Figure 13(*b*) shows the streamlines of the Gaussian vortex perturbed by the distortion $\varepsilon\Phi_1(r)\cos(2(\theta - w^{NL}t))$ computed in § 4 in the frame rotating at the angular frequency w^{NL}. The value $\varepsilon = 0.02$ has been chosen in order to obtain the best qualitative correspondence between the two plots since Rossi *et al.* (1997) did not provide the amplitude of the perturbation for the final state solution. The shapes of the streamlines for both solutions are surprisingly similar. Note that for their Reynolds number ($Re = 10^4$) and our ε, one has $\varepsilon^{3/2}Re \approx 28$ which is consistent with the nonlinear critical layer condition (4.6). A good agreement is also found for the angular frequency which is $w \approx 0.01$ in Rossi *et al.* (1997) and $w \approx 0.012$ in our calculation with their normalization ($\omega_{max} = 1/(4\pi + t/Re) \approx 0.075$ at $t = 500$). Rossi *et al.* (1997) also showed that their non-axisymmetric solution is rapidly eroded and modified when Re is divided by a factor 10. This could be associated with the appearance of viscous effects in the critical layer which in particular would explain the weak damping and the modification of the orientation of the distortion observed by Rossi *et al.* (1997). Unfortunately, Rossi *et al.* (1997) did not report results with higher Reynolds numbers. From the present study, one can conjecture that the threshold in perturbation amplitude for the existence of the non-axisymmetric state would decrease with increasing Reynolds numbers.

Dritschel (1998) also obtained long-lived non-axisymmetric vortex solutions by looking at the evolution of a compact region of vorticity which initially has an elliptical shape. He showed that the steeper the edge vorticity gradients, the more eccentric the vortex can remain. However, the existence of a stationary non-axisymmetric state of small eccentricity may be not related to the steepness of the edge gradients. In § 4, we indeed proved that there exist neutral non-axisymmetric perturbations with both 2-fold and 3-fold symmetries for vortices ranging from the Lamb vortex to the Rankine vortex. Moreover, for both cases, the nonlinearity needed for their existence, which can be measured, for a fixed Reynolds number, by the parameter h_c, was shown to be almost independent on the steep edge gradient parameter a (see figure 11*c*). By contrast, the linear viscous damping of the perturbation is strongly dependent on a (see figure 12*b*). More precisely, for weak damping, the viscous damping rate

is actually proportional to the vorticity gradient at the critical point, which, for our profiles, becomes exponentially small as a goes to 1. Therefore, one may conclude that steep edge gradients make viscous modes less stable but do not influence the existence of nonlinear modes. For the compact vortices considered by Dritschel (1998), one can show that the viscous damping of the linear perturbations of azimuthal wavenumber $m = 2$ is always null because the critical point is always outside the compact region of vorticity. This implies that there is no singularity at the critical point and thus no need of a critical layer. For these vortices, the nonlinear modes (i.e. the modes with a nonlinear critical layer) are then identical to the linear (viscous) modes. This also means that stationary non-axisymmetric states could exist as close as we wish to the axisymmetric state. This is indeed confirmed by Legras & Dritschel (1991) who obtained for similar compact vortices stable non-axisymmetric equilibria of aspect ratio close to 1. In this respect, the compact vortices studied in Legras & Dritschel (1991) and Dritschel (1998) are clearly different from the class of vortices studied here and in Bassom & Gilbert (1998) which are linearly asymptotically stable and thus for which the non-axisymmetric perturbation would have to be sufficiently large to survive.

6. Discussion

6.1. *Electron columns*

It is interesting to recast the results of §§ 3 and 4 in the context of columns of electrons (Briggs *et al.* 1970; Driscoll & Fine 1990). For two-dimensional columns of electrons, the governing equations are isomorphic to the two-dimensional Euler equations. The electronic potential corresponds to the streamfunction Ψ and satisfies (2.1) without the right-hand side. Briggs *et al.* (1970) were probably the first to explain the effects of vorticity gradients on the linear non-viscous spectrum of vortices. They showed that the discrete neutral modes of a piecewise vorticity profile are transformed into damped quasi-modes (i.e. non-regular) with a damping rate proportional (for small damping rates) to the vorticity gradient at the critical point. They demonstrated that this damping is related to the so-called Landau damping of uniform plasmas which is associated with a causality condition. In fact, it turns out that this damping is actually equal to what would have been obtained with weak viscous effects because both viscosity and causality prescribe the same procedure of integration above the critical point. It follows that the viscous eigenfrequencies given in figure 12 correspond to quasi-mode frequencies of a electron column with a mean density given by (4.1). Similarly, the nonlinear eigenmodes can also be recast in the electron columns framework as they do not directly involve viscosity.† They may correspond to the so-called trapped modes observed in the experiments of Driscoll & Fine (1990). The external strain field considered in § 3 has its equivalent in electron plasmas. It can be generated by either other electron columns or magnetic forcing (Driscoll & Fine 1990). Thus, the results of § 3 can also be applied in the context of electron columns. In particular, one expects distortions without critical layers (§ 3.1) or with a purely nonlinear critical layer to be similar in both cases. However, it is not clear whether the singular distortion associated with a viscous critical layer would be visible. Indeed, if the singularity is not smoothed by nonlinearity, it has to be smoothed by time-

† In fact, viscosity is necessary to get an equilibrium critical layer, even if the critical layer is purely nonlinear (Benney & Bergeron 1969). For electron columns, one expects that the critical layer would be in quasi-equilibrium: in that case, the phase jump across the nonlinear critical layer may be zero with a different inner structure (e.g. Goldstein & Leib 1988).

dependent effects. If this is possible, one expects other distortions, such as inertial waves, to be generated at the critical layer location, and presumably to be present everywhere. It would not be surprising if the spiral structure observed by Driscoll & Fine (1990) could be related to that effect.

6.2. *Transient effects*

Inertial waves, and therefore the spiral filaments associated with them, are also expected to be present during the transient regime to the stationary solution. No transients have been considered in the present analysis. They were considered in Bernoff & Lingevitch (1994) and Bassom & Gilbert (1998) for the simple two-dimensional linear unforced case. They showed that during the evolution from an arbitrary initial condition, strong transients characterized by the generation of inertial waves are present (Bernoff & Lingevitch 1994). These inertial waves eventually die on a $O(Re^{1/3})$ time scale everywhere except in the vortex centre where they become singular and generate an algebraically decreasing eigenmode (Bassom & Gilbert 1998).

In the linear regime, the presence of an external forcing does not modify this scenario. This means that if there is no critical layer or if the critical layer is purely viscous (i.e. $h \gg 1$), the non-axisymmetric correction created by the external field is not influenced by transients. It always appears after transients have died out even if it may take a very long time. However, as soon as nonlinear effects are present, transients may affect the non-axisymmetric correction. Indeed, transients are expected to be the most important in the critical layer. They change the nature of the critical layer which becomes time-dependent and consequently they also modify some essential properties such as the phase jump χ across the critical layer which defines the non-axisymmetric correction. Under certain conditions, the time-dependent critical layer may slowly evolve into an equilibrium critical layer as explained by Goldstein & Hultgren (1988), but this is not always the case. In particular, several other scenarii including finite time singularity have already been identified (see Cowley & Wu 1994, and references therein). Nevertheless, the good agreement obtained in § 5 between the stationary solution and the numerical solution obtained from an initial value problem (Rossi *et al.* 1997) reinforces the idea that a quasi-equilibrium critical layer regime can indeed be achieved, even in the unforced case.

6.3. *Summary*

In this paper, the non-axisymmetric correction to a Gaussian vortex generated by an additional rotating multipolar strain field has been calculated. This work extends Moffatt *et al.*'s (1994) analysis which only considered a stationary strain field. This extension is not trivial when the angular frequency of the external field is in the range of the angular velocity of the vortex due to the presence of a critical point singularity. We have resolved that singularity by the introduction of viscous and nonlinear effects and shown that the entire structure of the correction depends on the value of the Haberman parameter $h = h_c/(\varepsilon^{3/2}Re)$ which characterizes the nature of the critical layer. Both the scaling and the variation with respect to the angular frequency of the vorticity correction maximum have been determined. In the viscous critical layer regime, a good agreement has been found with the viscous numerical simulations by Lingevitch & Bernoff (1995). For a purely nonlinear critical layer ($h \ll 1$), we have demonstrated that the non-axisymmetric correction can survive without external field for specific angular frequencies when the perturbation azimuthal wavenumber is $n = 2$ and 3. The resulting non-axisymmetric vortex has been compared to the

numerical solutions obtained by Rossi *et al.* (1997) for $n = 2$ and a good agreement has been found.

The existence of such non-axisymmetric vortices in a strain-free environment has also been analysed for a continuous family of vorticity profiles ranging from Gaussian to top-hat (Rankine vortex). Nonlinear eigenmodes with azimuthal wavenumber $n = 2$ and 3 have been found to exist whatever the steepness of the vorticity profile. For larger azimuthal wavenumbers, we have shown that nonlinear eigenmodes exist only if the vorticity profile becomes sufficiently steep. The amplitude threshold of these modes has been determined as a function of the Reynolds number. Below this threshold, a non-axisymmetric correction with the same angular frequency survives only if an external field, which has been calculated is added. Otherwise, the non-axisymmetric correction is progressively eroded. When the viscous effect eventually becomes dominant, the correction is expected to evolve according to a linear viscous mode. Both the frequency and the damping rate of the linear viscous modes have been computed. An asymptotic expression for the damping rate has also been given for steep vorticity profiles. This has confirmed the importance of the vorticity gradient in the critical layer which was found to measure the 'gap' between the linear viscous mode and the nonlinear mode. In particular, it has been demonstrated that both modes tend to the well-known linear Kelvin modes as the vorticity profile tends to top-hat.

I would like to thank Alberto Verga for his comments on a preliminary version of the paper. The American Institute of Physics, Rossi, Lingevitch and Bernoff are acknowledged for having given permission to reproduce figure 13(*a*) from the paper Rossi *et al.* (1997). I am also grateful to L. Rossi who sent me the postscript file.

Appendix. Critical layer jumps and scalings

In this Appendix, the algebraic manipulations leading to the definitions of h and h_c are given. Basic results from Haberman (1972) and Smith & Bodonyi (1992) concerning the jumps across an equilibrium critical layer are presented. Expressions used in § 3.2 for the non-axisymmetric vorticity maximum are also given.

The distinguished scaling in the critical layer is obtained when both viscous and nonlinear effects are of same order, that is when $\varepsilon^{1/2}$ and $Re^{-1/3}$ are of same order. In that case, the critical layer singularity is resolved on a characteristic viscous-nonlinear scale $\delta = \sqrt{\varepsilon} = O(1/Re^{1/3})$.

In the frame rotating with the angular frequency w, the streamfunction outside the critical layer is

$$\Psi = \Psi_c - \int_{r_c}^{r} (\Omega_0(s) - w)s \, \mathrm{d}s + \varepsilon \mathrm{Re}\,(\Phi_1(r)\mathrm{e}^{\mathrm{i}n\theta}) + \cdots. \tag{A 1}$$

By examining this expression near $r = r_c$, one reaches the conclusion that the expansion for the streamfunction in the critical layer has the form (assuming without restriction $\Psi_c = 0$)

$$\Psi = \varepsilon\Psi_1(\tilde{r}, \theta) + \varepsilon^{3/2} \ln(\varepsilon)\Psi_2(\tilde{r}, \theta) + \varepsilon^{3/2}\Psi_3(\tilde{r}, \theta) + \cdots, \tag{A 2}$$

with $\tilde{r} \equiv r/\sqrt{\varepsilon}$.

The first two terms Ψ_1 and Ψ_2 are immediately obtained by rewriting the outer

solution with the local variable

$$\Psi_1 = -\frac{r_c\Omega'_{0_c}}{2}\tilde{r}^2 + \Phi_{1_c}\cos(n\theta), \quad \Psi_2 = -\frac{\omega'_{0_c}\Phi_{1_c}}{2r_c\Omega'_{0_c}}\tilde{r}\cos(n\theta), \tag{A 3}$$

where the suffix c indicates that values are taken at r_c.

The equation for Ψ_3 reads

$$\frac{\partial\Psi_1}{\partial\tilde{r}}\frac{\partial^3\Psi_3}{\partial\theta\partial\tilde{r}^2} - \frac{\partial\Psi_1}{\partial\theta}\frac{\partial^3\Psi_3}{\partial\tilde{r}^3} = \frac{r_c}{\varepsilon^{3/2}Re}\frac{\partial^4\Psi_3}{\partial\tilde{r}^4} + \frac{1}{r_c}\frac{\partial\Psi_1}{\partial\theta}\frac{\partial^2\Psi_1}{\partial\tilde{r}^2}, \tag{A 4}$$

i.e.

$$-\Omega'_{0_c}r_c\tilde{r}\frac{\partial^3\Psi_3}{\partial\theta\partial\tilde{r}^2} + n\Phi_{1_c}\cos(n\theta)\frac{\partial^3\Psi_3}{\partial\tilde{r}^3} = \frac{r_c}{\varepsilon^{3/2}Re}\frac{\partial^4\Psi_3}{\partial\tilde{r}^4} + n\sin(n\theta)\Phi_{1_c}\Omega'_{0_c}, \tag{A 5}$$

with the matching condition

$$\Psi_3 \sim (\Omega'_{0_c} - \omega'_{0_c})\frac{\tilde{r}^3}{6} + \frac{\omega'_{0_c}\Phi_{1_c}}{r_c\Omega'_{0_c}}\tilde{r}\ln|\tilde{r}|\cos(n\theta) \quad \text{as } r \to -\infty. \tag{A 6}$$

Using the following change of functions:

$$\Psi_3 = -\omega'_{0_c}\left|\frac{\Phi_{1_c}}{r_c\Omega'_{0_c}}\right|^{3/2}\overline{\Psi}_3 + \Omega'_{0_c}\frac{\tilde{r}^3}{6}, \quad R = \left|\frac{r_c\Omega'_{0_c}}{\Phi_{1_c}}\right|^{1/2}\tilde{r}, \quad X = n\theta, \tag{A 7}$$

we get a single parameter problem for $\overline{\Psi}_3$

$$R\frac{\partial^3\overline{\Psi}_3}{\partial X\partial R^2} + \sin(X)\frac{\partial^3\overline{\Psi}_3}{\partial R^3} = h\frac{\partial^4\overline{\Psi}_3}{\partial R^4}, \tag{A 8}$$

$$\overline{\Psi}_3 \sim \tfrac{1}{6}R^3 + R\ln|R|\cos(X) \quad \text{as } R \to -\infty, \tag{A 9}$$

with

$$h = \frac{|\Omega'_{0_c}|^{1/2}}{nRe}\left|\frac{r_c}{\varepsilon\Phi_{1_c}}\right|^{3/2}. \tag{A 10}$$

This problem was first studied by Haberman (1972), then re-examined and corrected by Brown & Stewartson (1978) and Smith & Bodonyi (1982). The conclusion they reached is that the behavior of $\overline{\Psi}_3$ for large R is of the form

$$\overline{\Psi}_3 \sim \tfrac{1}{6}R^3 + R\ln|R|\cos(X) + \eta(h)\tfrac{1}{2}R^2 + U(h,X)R \quad \text{as } R \to +\infty, \tag{A 11}$$

where $\eta(h)$ and $U(h,X)$ are vorticity and velocity jumps respectively. The velocity jump $U(h,X)$ is 2π-periodic with respect to X and can be written as

$$U(h,X) = \sum_{p=0}^{\infty}(U^{(p)}(h)\sin(nX) + V^{(p)}(h)\cos(nX)). \tag{A 12}$$

It follows that the phase jump appearing in (3.3) is given by

$$\chi(h) = -U^{(1)}(h) = -\frac{1}{\pi}\int_0^{2\pi}U(h,X)\sin(X)\mathrm{d}X. \tag{A 13}$$

Smith & Bodonyi (1982) computed the function $\chi(h)$ and obtained a result comparable to Haberman's calculation although the latter did not consider the harmonics in (A 12). Their result is reproduced in figure 14.

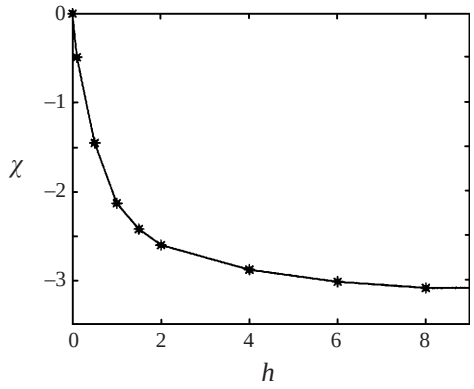

FIGURE 14. Sketch of the phase jump χ versus h (after Smith & Bodonyi 1982). The large-h asymptote of χ is $-\pi$.

Haberman (1972) showed that the vorticity jump $\eta(h)$ can be computed from $\chi(h)$ by the formula

$$\eta(h) = \frac{\chi(h)}{4h}. \tag{A 14}$$

For a given value of h ($\neq 0$), several harmonics are in general present in (A 12) and $\eta(h)$ is in general non-zero which means that in addition to the phase jump, the critical layer generates in the outer region an $O(\varepsilon^{1/2})$ axisymmetric correction as well as $O(\varepsilon)$ harmonic corrections.

For a purely viscous critical layer, Smith & Bodonyi (1982) proved that

$$U(h, X) \sim \pi \sin(nX) \quad \text{as } h \to \infty, \tag{A 15}$$

which guarantees that $\chi(h) \sim -\pi$ as $h \to \infty$ but also that the $O(\varepsilon)$ harmonic corrections and the $O(\varepsilon^{1/2})$ axisymmetric correction are absent in that limit. For a purely nonlinear critical layer ($h \ll 1$), they showed that $U(k, X) = O(h)$ which means the $O(\varepsilon)$ harmonic corrections are also negligible in that case. By contrast, the $O(\varepsilon^{1/2})$ axisymmetric correction does not disappear since the vorticity jump $\eta(h)$ goes to a constant. Smith & Bodonyi (1982) obtained the following estimates for $\chi(h)$ and $\eta(h)$:

$$\chi(h) \sim -4Ch \quad \text{as } h \to 0, \tag{A 16}$$

$$\eta(h) \sim -C \quad \text{as } h \to 0, \tag{A 17}$$

with $C \approx 1.3$.

The implications of these results can be summarized as follows. Although there may exist corrections of same order or larger, the streamfunction of the fundamental distortion is perfectly defined in the outer region by equations (2.5) and (3.3). The only relevant quantity from the critical layer that intervenes in its definition is the phase jump $\chi(h)$ which is sketched in figure 14. However, expansion (2.3) is in principle not an approximation of the total field as $O(\varepsilon^{1/2})$ terms generated by the critical layer should be taken into account. The only exception is for viscous critical layers.

In the frame rotating with the angular frequency w, the vorticity field in the critical layer has the following expansion:

$$\omega(\tilde{r}, \theta) = -r_c \Omega'_{0_c} + \sqrt{\varepsilon}\tilde{r}\Omega'_{0_c} + \sqrt{\varepsilon}\omega_3(\tilde{r}, \theta) + \cdots \tag{A 18}$$

with

$$\omega_3 = -\omega'_{0_c} \left| \frac{\Phi_{1_c}}{r_c \Omega'_{0_c}} \right|^{1/2} \frac{\partial^2 \overline{\Psi}_3}{\partial R^2} \tag{A 19}$$

where $\overline{\Psi}_3$ is defined by (A 8) and (A 9). If one decomposes the vorticity field as

$$\omega(\tilde{r}, \theta) = \sum_{p \geqslant 0} \gamma^{(p)}(\tilde{r}) \cos(pn\theta) + \mu^{(p)}(\tilde{r}) \sin(pn\theta),$$

the amplitude $\gamma^{(1)}$ of the fundamental distortion has a maximum in the critical layer which can be written as

$$\omega^{(1)}_{max}(h, w, n) = |\omega'_{0_c}| \left| \frac{\Phi_{1_c}}{r_c \Omega'_{0_c}} \right|^{1/2} M^{(1)}(h) \sqrt{\varepsilon}, \tag{A 20}$$

where

$$M^{(1)}(h) = \max_{R\text{real}} \left| \frac{1}{\pi} \int_0^{2\pi} \frac{\partial^2 \overline{\Psi}_3}{\partial R^2} \cos(\tilde{X}) \mathrm{d}\tilde{X} \right|. \tag{A 21}$$

Similarly, the maximum ω^{NA}_{max} of non-axisymmetric part of the vorticity is also given by expression (A 20) where $M^{(1)}$ is replaced by

$$M(h) = \max_{X \in (0,2\pi); R\text{real}} \left| \frac{\partial^2 \overline{\Psi}_3}{\partial R^2} - \frac{1}{2\pi} \int_0^{2\pi} \frac{\partial^2 \overline{\Psi}_3}{\partial R^2} \mathrm{d}\tilde{X} \right|. \tag{A 22}$$

When the correction of the streamfunction is normalized in the vortex centre, Φ_{1_c} is perfectly defined by the linear inviscid equation (2.5). In that case, the non-axisymmetric vorticity maximum depends on h only through the factor $M(h)$. In other words, the variations of the vorticity maximum with respect to w and n are the same for any fixed h and ε.

Using expression (A 10), ω^{NA}_{max} can also be written as

$$\omega^{NA}_{max} = |\omega'_{0_c}| \frac{|\Phi_{1_c}|}{|r_c| |\Omega'_{0_c}|^{2/3}} (nRe)^{1/3} h^{1/3} M(h) \varepsilon. \tag{A 23}$$

In the viscous regime ($h \to \infty$), the maximum of the non-axisymmetric vorticity is also the maximum of the fundamental distortion $\omega^{(1)}_{max}$ and $h^{1/3} M(h)$ goes to a non-zero constant $M_v = \max_{R\text{real}} |\mathrm{Re}(\tilde{\omega}_3)|$ where $\overline{\omega}_3$ satisfies the viscous critical layer equation

$$\frac{\partial^2 \overline{\omega}_3}{\partial R^2} - R\, \overline{\omega}_3 = 1, \tag{A 24}$$

with

$$\overline{\omega}_3 \sim -\frac{1}{R} \quad \text{as } R \to \pm\infty. \tag{A 25}$$

Some properties of the function $\overline{\omega}_3$, can be found in the appendix of Drazin & Reid's (1981) textbook.

REFERENCES

Bassom, A. P. & Gilbert, A. D. 1998 The spiral wind-up of vorticity in an inviscid planar vortex. *J. Fluid Mech.* **371**, 109–140.

Benney, D. J. & Bergeron, R. F. 1969 A new class of nonlinear waves in parallel flows. *Stud. Appl. Maths* **48**, 181–204.

Bernoff, A. J. & Lingevitch, J. F. 1994 Rapid relaxation of an axisymmetric vortex. *Phys. Fluids* **6**, 3717–3723.

Briggs, R. J., Daugherty, J. D. & Levy, R. H. 1970 Role of Landau damping in cross-field electron beams and inviscid shear flow. *Phys. Fluids* **13**, 421–432.

Brown, S. N. & Stewartson, K. 1978 The evolution of the critical layer of a Rossby wave. Part II. *Geophys. Astrophys. Fluid Dyn.* **10**, 1–24.

Cowley, S. J. & Wu, X. 1994 Asymptotic approaches to transition modelling. *AGARD Rep.* 793, pp. 3.1–3.38.

Drazin, P. G. & Reid, W. H. 1981 *Hydrodynamic Stability*. Cambridge University Press.

Driscoll, C. F. & Fine, K. S. 1990 Experiments on vortex dynamics in pure electron plasmas. *Phys. Fluids* B **2**, 1359–1366.

Dritschel, D. G. 1995 A general theory for two-dimensional vortex interactions. *J. Fluid Mech.* **293**, 269–303.

Dritschel, D. G. 1998 On the persistence of non-axisymmetric vortices in inviscid two-dimensional flows. *J. Fluid Mech.* **371**, 141–155.

Goldstein, M. A. & Hultgren, L. S. 1988 Nonlinear spatial evolution of an externally excited instability wave in a free shear layer. *J. Fluid Mech.* **197**, 295–330.

Goldstein, M. A. & Leib, S. J. 1988 Nonlinear roll-up of external excited free shear layers. *J. Fluid Mech.* **191**, 481–515.

Haberman, R. 1972 Critical layers in parallel flows. *Stud. Appl. Maths* **51**, 139–161.

Hopfinger, E. J. & Heijst, G. J. F. van 1993 Vortices in rotating fluids. *Ann. Rev. Fluid Mech.* **25**, 241–289.

Jiménez, J., Moffatt, H. K. & Vasco, C. 1996 The structure of the vortices in freely decaying two-dimensional turbulence. *J. Fluid Mech.* **313**, 209–222.

Legras, B. & Dritschel, D. G. 1991 The elliptical model of two-dimensional vortex dynamics. I: The basic state. *Phys. Fluids* A **3**, 845–854.

Levy, R. H. 1965 Diocotron instability in a cylindrical geometry. *Phys. Fluids* **8**, 1288–1295.

Lin, C. C. 1955 *The Theory of Hydrodynamics Stability*. Cambridge University Press.

Lingevitch, J. F. & Bernoff, A. J. 1995 Distortion and evolution of a localized vortex in an irrotational flow. *Phys. Fluids* **7**, 1015–1026.

Lundgren, T. S. 1982 Strained spiral vortex model for turbulent fine structure. *Phys. Fluids* **25**, 2193–2203.

Maslowe, S. A. 1986 Critical layers in shear flows. *Ann. Rev. Fluid Mech.* **18**, 405–432.

McWilliams, J. C. 1984 The emergence of isolated coherent vortices in turbulent flow. *J. Fluid Mech.* **146**, 21–43.

Melander, M. V., McWilliams, J. C. & Zabusky, N. J. 1987 Axisymmetrization and vorticity-gradient intensification of an isolated two-dimensional vortex through filamentation. *J. Fluid Mech.* **178**, 137–159.

Mitchell, T. B. & Driscoll, C. F. 1994 Symmetrization of 2D vortices by beat-wave damping. *Phys. Rev. Lett.* **73**, 2196–2199.

Moffatt, H. K., Kida, S. & Ohkitani, K. 1994 Stretched vortices – the sinews of turbulence; large-Reynolds-number asymptotics. *J. Fluid Mech.* **259**, 241–264.

Moore, D. W. & Saffman, P. G. 1971 Structure of a line vortex in an imposed strain. In *Aircraft Wake Turbulence* (ed. Olsen, Golburg & Rogers), pp. 339–354. Pleum.

Rossi, L. F., Lingevitch, J. F. & Bernoff, A. J. 1997 Quasi-steady monopole and tripole attractors for relaxing vortices. *Phys. Fluids* **9**, 2329–2338.

Saffman, P. G. 1992 *Vortex Dynamics*. Cambridge University Press.

Schecter, D. A., Dubin, D. H. E., Lansky, I. M. & O'Neil, T. M. 1998 Eigenmode analysis of the inviscid growth and decay of small perturbations on a two-dimensional axisymmetric vortex. Submitted to *Phys. Fluids*.

Smith, F. T. & Bodonyi, R. J. 1982 Nonlinear critical layers and their development in streaming-flow stability. *J. Fluid Mech.* **118**, 165–185.

Ting, L. & Tung, C. 1965 Motion and decay of a vortex in a nonuniform stream. *Phys. Fluids* **8**, 1039–1051.